

Boundary Physics Part II: To the Window, To the Wall

Lecture by Chairman Professor Dr. G.R. Tynan

Summary by R. Masline

June 7, 2021



Study of the edge is highly interdisciplinary [1].

Contents

1	Sketch of the "Problem"	1
1.1	Schematic of the edge	1
1.2	Scaling estimates	2
1.2.1	Density scale length	3
1.2.2	Temperature scale length	4
1.2.3	Pressure scale length	5
1.2.4	Parallel heat flux	5
2	PMI: Effect of materials on the plasma	7
2.1	Open field line zone - the SOL	7
2.2	Plasma sheaths	8
2.2.1	Implications	9
2.2.2	Sheath dissipation effect	9
2.2.3	Profile variation across LCFS	11
3	PMI: Effect of plasma on the materials	12
3.1	What's going on?	12
3.2	Where PMI comes in	13
3.2.1	Divertor particle and power handling	13
3.2.2	PMI impact on confinement	16
3.2.3	Surface morphology evolution	16
3.2.4	Helium accumulation	17

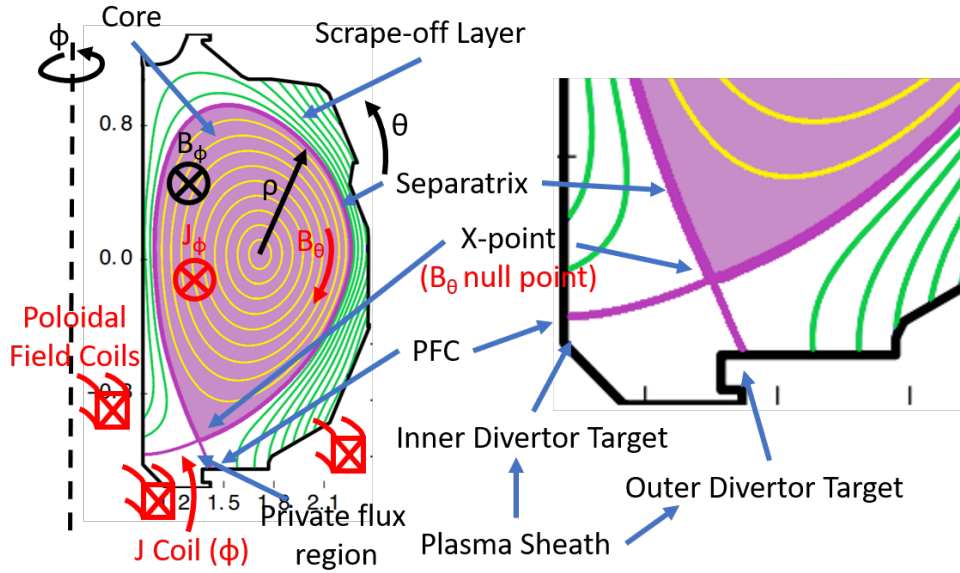


Figure 1: Cartoon of a tokamak plasma, focusing on the edge region. The plasma is in purple, the vacuum is white, and the material surfaces are shown in the black outline. Red annotations denote magnetics, while black annotations denote coordinates. Closed field lines are shown in yellow, open field lines are shown in green, and the last closed flux surface (separatrix) is shown in dark purple.

1 Sketch of the "Problem"

This discussion is focused on the tokamak, but similar concepts apply for stellarators and other magnetic confinement systems.

1.1 Schematic of the edge

The geometry of the tokamak is shown in Figure 1.

The axis of symmetry for the torus is on the left. The solid black line represents the first wall of the tokamak. Both the toroidal magnetic field (B_ϕ) and toroidal current density (J_ϕ) are both into the paper. The yellow, green, and thick dark purple lines in the figure are magnetic flux surfaces. The yellow lines are closed magnetic flux surfaces, while the green lines are open magnetic flux surfaces that peel away from the plasma and touch the divertor target or the walls of the device. The thick purple line is the last closed flux surface (LCFS), or the "separatrix", that separates the regions of open and closed magnetic field lines that has a null point where it crosses itself, called the X-point. This X-point is formed by special poloidal field coils, called shaping coils. These poloidal field coils run a current through the coil that is parallel to the main plasma current, which creates a null in the magnetic field at the X-point. At this point, the poloidal field vanishes, and there is finite poloidal field throughout the rest of the system. There can be one X-point at the bottom or the top of the device, two X-points at the top and bottom, or multiple X-points throughout the device. The

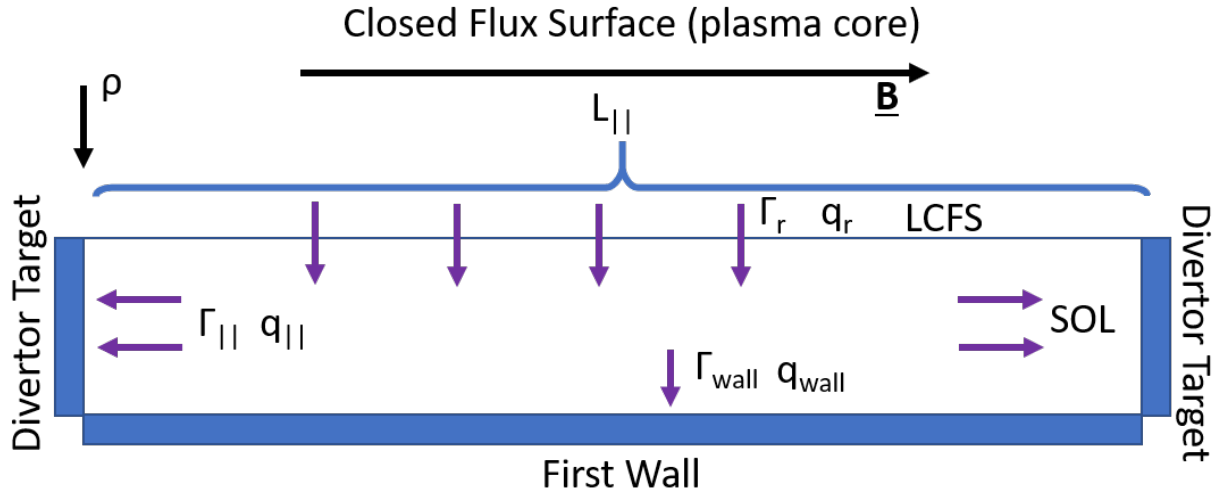


Figure 2: Alternative view of the last-closed flux surface, core, and SOL, where the edge of the plasma has been "peeled off" the tokamak and flattened into new coordinates. These new coordinates show the poloidal direction as the horizontal axis and the radial direction as the vertical axis. The field line terminates at each of the two divertor targets. Fluxes are drawn as purple arrows.

plasma can be shaped, stretched, and pulled into these different shapes for different reasons, often to improve MHD stability or heat dissipation.

The open field lines that intersect the material surfaces form what is called the "scrape-off layer", which is all the plasma in the region outside of the LCFS. Most modern-day tokamaks operate using a so-called "divertor" geometry, but older incarnations of tokamaks would run with limiters, which are material objects shoved into the plasma that come directly into contact with the LCFS, which caused intense impurity contamination of the plasma from the erosion of the limiter and strong buildup of neutral gas from recycling (neutralization) of the plasma on the limiter surface. Limiters degrade performance are no longer used.

The scrape-off layer region encompasses the area where the plasma interacts with material surfaces, which include the divertor targets and the walls of the machine. In this region, the interactions between the intense plasma and the material surface are complex - the materials themselves can influence the behavior of the plasma (like how the limiter configuration degraded plasma performance), and the plasma also has an effect on the materials (like how the plasma erodes the limiter).

1.2 Scaling estimates

The geometry of the SOL is rather complex, and a simplified version is shown in Figure 2. This structure shows the poloidal direction as the horizontal axis and the radial direction as the vertical axis, as though the SOL were "peeled off" the poloidal section and flattened out, from divertor target to divertor target. The symbol ρ is the normalized magnetic flux, going from 0 at the magnetic

axis to 1 at the LCFS. The boundaries are defined by the divertor targets in the poloidal/horizontal direction, and the LCFS at the upper boundary and the first wall at the lower boundary in the vertical direction. Between these regions is the SOL.

Plasma ionization and plasma heating usually occur in the core. This creates an influx of particles and heat from the core plasma into the SOL, γ_r and q_r , respectively. The core plasma is fueling the scrape off layer across the LCFS. Once the plasma reaches the SOL region, a new phenomena can occur: parallel flow can bring the particles along the lines of the magnetic field (in the horizontal direction, in this sketch) and the plasma will flow into the divertor target plates. The flux can also travel across the magnetic surface. Some makes it to the wall, but the rest of it is swept through by the parallel flow and into the divertor target. The cross-field flux is usually represented as a turbulent flux,

$$\Gamma_r \simeq \langle \tilde{n} \tilde{v}_r \rangle + \Gamma_r^{\text{neo}}, \quad (1)$$

where $\langle \tilde{n} \tilde{v}_r \rangle$ is a time average or a poloidal surface average of the density fluctuation times the radial velocity fluctuation, and maybe a neoclassical contribution Γ_r^{neo} from trapped particles. The heat flux

$$q_{e,ir} \simeq \frac{3}{2} T_{e,i} \langle \tilde{n} \tilde{v}_r \rangle + \frac{3}{2} n_{e,i} \langle \tilde{T}_{e,i} \tilde{v}_r \rangle + q_{e,ir}^{\text{neo}}, \quad (2)$$

where the first term accounts for the convection piece of the heat flux, where the particles carry a finite amount of energy, the second term represents a conduction piece due to the correlations between the velocity fluctuations and the temperature fluctuations, and the third term can account for the neoclassical component of the heat flux. Usually, the turbulent contributions are much larger than the neoclassical contribution.

1.2.1 Density scale length

Once plasma crosses into the SOL, what happens to the plasma profiles, $n(r)$, $T(r)$...? We can use this sketch to determine how far the plasma extends into the scrape-off layer by applying some trivial analyses. First, start with particles. At steady state, the equation for particle conservation will be

$$\frac{\partial n}{\partial t} + \vec{\nabla} \cdot \vec{\Gamma} = S_{\text{ion}} - R_{\text{recomb}}, \quad (3)$$

assuming ionization and recombination are small enough to eliminate the plasma source and sink (this is an unrealistic assumption, but makes life easy and gets the point across). This gives $\vec{\nabla} \cdot \vec{\Gamma} = 0$, or, for this geometry,

$$\partial_r \Gamma_r = -\partial_{||} \Gamma_{||} \quad (4)$$

where the radial component balances with the parallel component. Then, we will naively assume that the cross-field, radial flux is diffusive,

$$\Gamma_r = -D_{\text{turb}} \nabla_r \bar{n} \sim -D_{\text{turb}} \frac{\bar{n}}{\lambda_n^2}, \quad (5)$$

where \bar{n} exponentially decays as $n \sim n_o e^{-r/\lambda_n}$, where n_o is the separatrix density. Note that this assumption is incorrect; cross-field SOL transport isn't diffusive and the majority of cross-field SOL transport is convective, with a ballistic or intermittent nature. However, these processes can be lumped in to an effective turbulent diffusivity for the purposes of this derivation.

The parallel flux is convective, with

$$\Gamma_{\parallel} \simeq \alpha n c_s, \quad (6)$$

where c_s is the ion acoustic speed and α as a scale factor, ranging from $0 < \alpha < 1$. The parallel gradient length for this problem is $\nabla_{\parallel} \sim 1/L_{\parallel} \sim 1/qR_o$. The scale L_{\parallel} is the connection length along the field lines between the target plates, shown in Figure 2. Equating the radial and parallel fluxes given in Eq. (5) and Eq. (6),

$$-D_{\text{turb}} \frac{\bar{n}}{\lambda_n^2} = -\frac{\alpha n c_s}{qR_o} \Rightarrow \lambda^2 = \frac{D_{\text{turb}} q R_o}{\alpha c_s}. \quad (7)$$

For typical experimental parameters $R_o \sim 4 \text{ m}$, $D_{\text{turb}} \sim 1 \text{ m}^2/\text{sec}$, $q \sim 3$, $\alpha \sim 0.5$, and $c_s \sim 10^5 \text{ m/sec}$, the density profile scale length works out to be about $1.4 \times 10^{-2} \text{ m}$. This means that the density profile in the SOL is on the order of a centimeter.

1.2.2 Temperature scale length

The argument for the temperature scale length is similar, but slightly different. Here, we assume a steady-state heat equation,

$$\vec{\nabla} \cdot \vec{q}_{e,i} = \cancel{Q_{e,i}} - \cancel{R_{\text{rad},e,i}}, \quad (8)$$

where the source and sink terms for heat and radiation are taken to be zero, for simplicity. The radial and parallel components of the heat flux are

$$q_{r \ e,i} \sim -n \chi_{i,e}^{\text{turb}} \nabla_r T_{i,e} \quad (9)$$

$$q_{\parallel \ i,e} \sim -n \chi_{\parallel} \nabla_{\parallel} T_{i,e}, \quad (10)$$

where $\chi_{||}$ is the Spitzer classical collisional resistivity, with $\chi_{||} \gg \chi_{i,e}^{\text{turb}}$. The temperature scales as $T \sim T_o e^{-r/\lambda_T}$, where T_o is the separatrix temperature, so

$$-n\chi_{i,e}^{\text{turb}} \frac{T}{\lambda_T^2} = -\frac{n\chi_{||}T}{qR_o} \Rightarrow \lambda^2 = \frac{\chi_{i,e}^{\text{turb}} qR_o}{\chi_{||}}. \quad (11)$$

For typical experimental parameters $R_o \sim 4 \text{ m}$, $\chi_{i,e}^{\text{turb}} \sim 1 \text{ m}^2/\text{sec}$, $q \sim 3$, and $\chi \sim$ Spitzer conductivity (which is not always true, but is a good estimate), the temperature profile scale length works out to be about on the order of a centimeter, like the density profile scale length.

1.2.3 Pressure scale length

The pressure profile is proportional to the heat flux, $P \propto nT$, and scales as

$$\frac{1}{\lambda_P} \sim \frac{1}{\lambda_n} + \frac{1}{\lambda_T} \sim \frac{\lambda_n \lambda_T}{\lambda_n + \lambda_T}, \quad (12)$$

and given our previous estimates, will be on the order of less than one centimeter.

1.2.4 Parallel heat flux

Now, we will estimate the parallel heat flux in the open field line region. In the core, the power from the core is equal to the radial heat flux escaping across the last closed flux surface,

$$f_\alpha Q_{\text{fusion}} + Q_{\text{aux}} = q_r S_{\text{LCFS}}, \quad (13)$$

where Q_{fusion} is the fusion power being produced in the core, f_α is the fraction of energy released in the alpha particles, Q_{aux} is the auxiliary heating (which we will neglect), q_r is the radial heat flux escaping from the core into the SOL and assumed uniform, and S_{LCFS} is the surface area of the last closed flux surface. The surface area of the LCFS is approximately $S_{\text{LCFS}} \sim 2\pi R_o 2\pi a \kappa$, where κ is the elongation. Plugging everything in, we see that

$$f_\alpha Q_{\text{fusion}} = q_r 4\pi^2 R_o a \kappa \Rightarrow q_r = \frac{f_\alpha Q_{\text{fusion}}}{4\pi^2 R_o a \kappa}. \quad (14)$$

This neglects radiation and other effects, which would constitute a ~ 2 factor correction. With $R_o \sim 4 \text{ m}$, $a \sim 1 \text{ m}$, $\kappa \sim 2$, $f_\alpha \sim 0.2$, and $Q_{\text{fusion}} = 500 \text{ MW}$, the radial heat flux crossing into the LCFS is approximately $3 \times 10^5 \text{ W/m}^2$.

To estimate the heat flux, we will use the geometry sketched in Figure 3. The plasma turbulence is carrying the heat flux q_r^{LCFS} to the LCFS, and it flows (in the parallel direction) to the target.

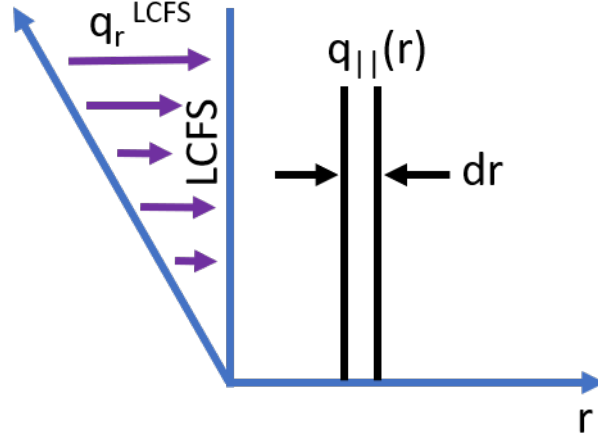


Figure 3: Radial and parallel heat fluxes across the LCFS.

A simple heat balance shows that the heat flux across the LCFS is equal to the parallel heat flux integrated across a radial profile,

$$\int_{S_{LCFS}} \vec{q}_r \cdot d\vec{s} = \int_{r=r_{LCFS}=0}^{\infty} q_{||}(r) dr \cdot 2\pi a \kappa, \quad (15)$$

assuming $q_{||}$ is uniform with respect to θ in the poloidal and toroidal direction. Like the density and temperature, we can assume that the heat flux decays exponentially, as $q_{||} \sim q_{||}^{LCFS} e^{-r/\lambda_p}$, so the heat balance expression becomes

$$f_\alpha Q_{\text{fusion}} = q_{||}^{LCFS} \int_{r=0}^{\infty} e^{-r/\lambda_p} dr \cdot 2\pi a \kappa \Rightarrow f_\alpha Q_{\text{fusion}} = 2\pi a \kappa q_{||}^{LCFS} \lambda_p, \quad (16)$$

meaning that the parallel heat flux can be written as

$$q_{||}^{LCFS} \simeq \frac{f_\alpha Q_{\text{fusion}}}{2\pi a \kappa \lambda_p}. \quad (17)$$

Using the same representative values as before, with $\lambda_p \sim 0.5\text{cm}$, we can see that the ballpark estimate for the parallel heat flux is approximately $1.6 \times 10^9 \text{W/m}^2$. For reference, the heat flux experienced during re-entry into Earth's orbit is approximately 3MW/m^2 , while a cutting torch or arc welder can reach heat fluxes of $10\text{-}100 \text{MW/m}^2$ - so we have at least 10-100 times more heat parallel heat flux at the outside midplane than a device specifically used to cut metal. No solid material will survive such a heat flux, so something must be done.

How can we reduce this heat flux? There are several options:



Figure 4: When someone asks you about the heat flux width at the midplane [6].

1. **Expand the flux surfaces in the SOL before they get to the target.** This is essentially "de-focusing" the plasma, where what was once a 5mm width at the midplane can become 5-50cm at the target, see Figure 4.
2. **Distribute heat over a larger area, via flux expansion or dissipation.**
 - (a) Radiation recombination (dissipative or detached divertor) [2–4], where a gas is introduced into the divertor plasma and undergoes inelastic collisions with the plasma electrons, radiating heat in 4π directions
 - (b) Increase R_o , q , which increase λ_n , λ_T , and λ_P , or use a grazing incidence angle of the magnetic field along the target to flare out the heat flux (alternative divertors, like Super-X or Snowflake, and negative triangularity) [5] that takes advantage of geometric properties to spread out the heat flux naturally

2 PMI: Effect of materials on the plasma

2.1 Open field line zone - the SOL

As we have seen, the open field lines in the SOL carry immense heat and particle fluxes. There are enormous heat fluxes to the divertor targets, and some of the plasma will make it to the first wall, although the radial heat fluxes to the first wall will be much, much lower than the parallel heat flux to the divertor targets. There are also high particle fluxes to the divertor target; the atoms on the divertor target are impacted by ions from the plasma approximately once every microsecond, meaning the surface of the divertor target is under constant bombardment from plasma ions and the target surface will be damaged as a result.

2.2 Plasma sheaths

The plasma sheath is a region directly next to the material target, between the plasma and the material surface. Here, the dynamics of the plasma change as electrons (which have a much higher thermal speed than ions, since they are lighter) rush towards and impact the material surface. To maintain ambipolarity of the plasma flow, a plasma sheath will form, where ions are accelerated by this electric field towards the target. This region is characterized by a strong electrostatic field, which will repel most of the free-streaming electron flux and attract ions to fall towards the target. A cartoon of the electric field configuration near the material surface is shown in Figure 5.

Full derivations of the plasma sheath equations can be found in [3], and more details for die-hard sheath enthusiasts can be found in [7], [8], and [9].

The basic model of the sheath assumes that the ions flowing towards the surface are collisionless, and the kinetic energy of the ions will be conserved as they fall down a potential profile. If a material surface is on the righthand side in Figure 5, the magnetic field will be going from left to right. Near the plasma edge, there is a potential drop that is very weak in the main plasma and drops off very steeply in a very thin layer close to the target, marked by the blue dashed line in the figure. The thickness of this plasma sheath is 10 Debye lengths, or 10s of microns in a fusion-grade plasma. The so-called "pre-sheath", where the potential drops weakly, can extend a few centimeters or up to a half a meter into the main plasma. The ions will get drawn towards the edge by the weak potential drop in the pre-sheath, and travel along towards the target as the potential drop becomes greater and greater until it hits the sheath region, where it is accelerated into the target. The potential profile in the sheath region must satisfy the nonlinear differential equation

$$\frac{d^2\Phi}{dx^2} = \frac{en_e}{\epsilon_0} \left[\exp\frac{\Phi}{T_e} - \left(1 - \frac{\Phi}{\frac{1}{2}Mu_s^2}\right)^{-1/2} \right]. \quad (18)$$

For a stable sheath to exist, the ions must enter the sheath region at the ion acoustic speed, meaning they will become supersonic as they accelerate through the sheath and into the target. They will strike the surface with a certain energy, that is proportional to the electron temperature. Typically, in a fusion-grade hydrogen plasma, this potential drop is approximately 3 times the electron temperature.

The existence of this sheath provides the boundary conditions for the SOL. Our derivation of the plasma density scale length assumed an exponentially decaying density in the radial direction, per the Boltzmann relation. When we assumed that there was convective, parallel transport along the field lines, that is because the plasma is free to move along the field lines as it approaches the divertor target, where it is accelerated and then terminates into the target with some energy. This is consistent with the radial decay of the density profile: because of particle conservation (there is no ionization, so there is no plasma source) and ions being pulled out of the bulk plasma and accelerated into the target, the density decays in the radial direction as a manifestation of the flows induced by the sheath. The change in the density in this region is approximately one half of the upstream density, which is observed in experiment and predicted in the sheath derivation equation.

2.2.1 Implications

There are several implications of the plasma sheath that are critical to understanding the dynamics of the edge plasma:

1. $\bar{v}_{||} \simeq c_s$ at the pre-sheath boundary
2. $\Delta\phi \simeq kT_e$; $k \sim 3$ for H plasmas. This means that the ions hit the surface with a few times the electron temperature as directed kinetic energy. In a fusion plasma, the ions will hit the surface with ~ 100 eV of kinetic energy.
3. Sheath introduces a new dissipation for parallel electron motion. From drift wave theory, we know that parallel electron dissipation plays a critical role in setting up the cross-phase relationship between density and potential fluctuations, or density and velocity fluctuations. The introduction of this new dissipation in the open line region drastically changes the physics of the edge turbulence - changing everything we have learned about electron drift waves or collisionless drift waves or CTEM in the closed line region because of this new dissipative term. The new term can drive these drift waves more virulently, and also allow for a new, so-called "interchange" instability that can occur on open field lines.
4. Since $\Delta\phi_{sheath} = kT_e$, and $T_e = T_e(r)$, $\Delta\phi_{sheath} = \Delta\phi_{sheath}(r)$

2.2.2 Sheath dissipation effect

The pre-sheath sets up the conditions of the problem such that the time-averaged current $\bar{J}_{||} = 0$, meaning the plasma is not charging up and exists in equilibrium. However, if there are potential and density fluctuations (where $\phi = \bar{\phi} + \tilde{\phi}$ and $n = \bar{n} + \tilde{n}$, respectively, where the twiddle-terms are fluctuations due to turbulence). The presence of these fluctuations means that the potential profile will oscillate up and down slightly, from the pre-sheath region through the sheath, relative to the constant zero potential at the material surface, shown as the dashed red lines along the potential profile in Figure 5. This means that at the sheath edge, the potential profile can go up and down, and a perturbation analysis of the electron current at the sheath shows that you can now have an oscillating current at the sheath edge that will be related to the potential and density fluctuations at the edge:

$$\nabla_{||}\tilde{J}_{||} = \frac{kT_e}{e\eta} \nabla_{||}^2 \left(\frac{\tilde{\phi}}{kT_e} - \frac{\tilde{n}}{n} \right), \quad (19)$$

for small $e\tilde{\phi}/kT$, \tilde{n}/n .

The key takeaway here is that the presence of the sheath introduces a new form of parallel electron dissipation, and we know that parallel electron dissipation is important in setting up the cross-phase in the models of electron drift waves that we have studied. It also allows the fluctuations to develop a parallel wave number that is very small. A plot of the potentials along the field line, terminating in both divertor targets, is shown in Figure 6. If the potential could not fluctuate, the potential would not change along the field line, as the blue line in the figure. If the potential could fluctuate and the fluctuation were fixed at zero at the sheath, then a fluctuation in the potential would have to have a node, as the purple line in the figure, where $k_{||} \sim 1/L_{||}$. If finite fluctuations in the potential

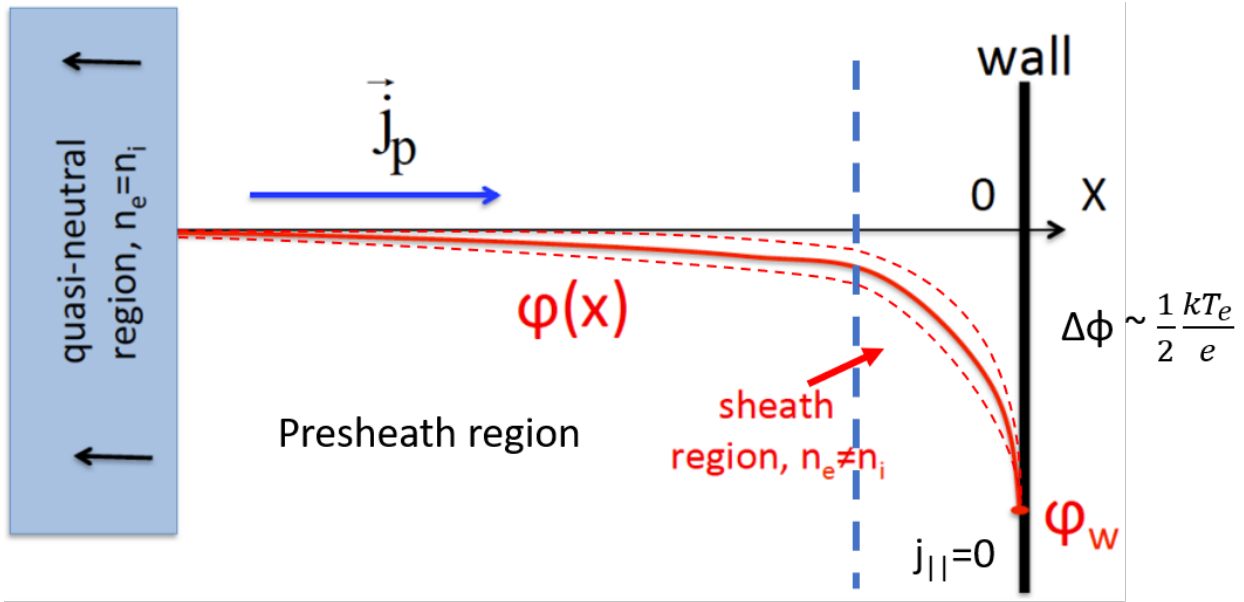


Figure 5: Cartoon of the plasma sheath. The potential drop is shown in the red solid line, while the dashed red lines represent the fluctuations in the potential. The quasi-neutral, presheath, and sheath regions are shown. Figure modified from [10].

exist and do not have to be zero at the end of the field line (which is the reality), the fluctuation is of order zero, $k_{||} \sim 0$, much smaller than it would be if there were zero fluctuations at the sheath edge.

This fact allows for the interchange, as opposed to the closed field line regions, where $k_{||}$ has to be periodic on the closed field lines and does not allow for the interchange mode to exist. The interchange only occurs in the SOL, and is thought to be a major player in SOL turbulence and transport.

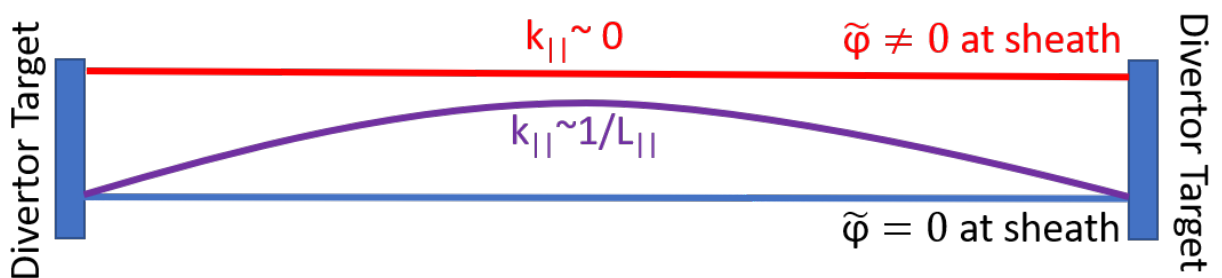


Figure 6: Potential profiles with and without fluctuations in the scrape-off layer, where each divertor target has a plasma sheath.

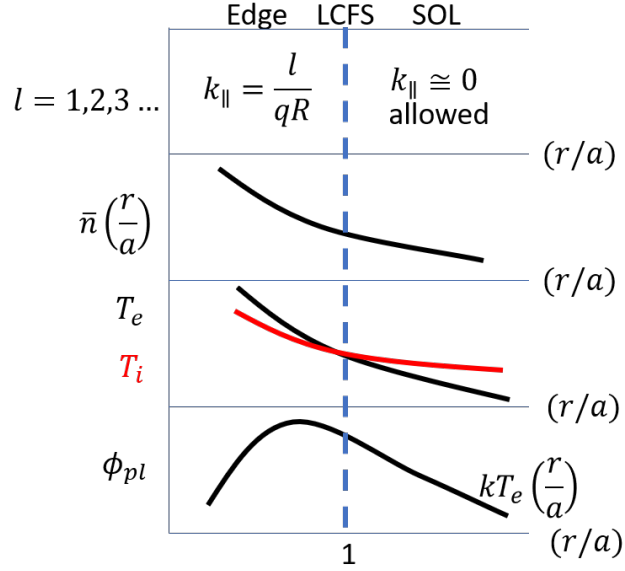


Figure 7: Plasma profiles at the edge plasma, LCFS, and SOL. The separatrix is located at $r/a = 1$.

2.2.3 Profile variation across LCFS

Now, we can look at the consequence of this plasma sheath in terms of profile variation across the separatrix, over the transition between the edge plasma and SOL. In the edge plasma region, where closed field lines are, is separated from the SOL, where the open field lines are, by the last closed flux surface, shown in Figure 7.

In the edge, k_{\parallel} is finite, where l is some integer and qR is the typical connection length along the magnetic field line in the closed field line region. This forces drift waves to be the dominant trigger for turbulence, particularly in a cold ion discharge (like an ohmic discharge). In the SOL, you can have finite k_{\parallel} , but it can also be very small or almost zero.

The density and temperature scale lengths in the scrape off layer have been estimated earlier, and are shown in the figure.

The structure of the potential profile is determined by the plasma sheath. As mentioned previously, the sheath potential is proportional to the electron temperature at any given flux surface. That means that in the open field line regions, the plasma potential will look as it does in the figure - monotonically decreasing towards the target sheath potential, meaning the electric field will point in the outward direction. Inside the LCFS, the behavior of the potential can be determined by looking at the radial component of the ion momentum equation,

$$m_i n \left(\frac{\partial}{\partial t} + \vec{v} \cdot \nabla \right) \vec{v}_r = qnE_r - \nabla P_i + \vec{v}_i \times \vec{B} + \dots \quad (20)$$

If the plasma flows are small (in situations of really strong flow damping, or low temperature tokamak plasmas), then the terms in the pressure balance cancel to leave only $E_r = \nabla P_i / qn < 0$

for $r/a < 1$. The radial electric field will be negative in this zone, which accounts for the behavior of the potential in the edge, shown on the graph. Since the radial electric field increases towards the plasma sheath, we see that the radial electric field changes sign somewhere around the LCFS. A change in the radial electric field gives rise to a guiding center $\vec{v}_{\vec{E} \times \vec{B}}$ drift, giving a radial gradient $\partial \vec{v}_{\vec{E} \times \vec{B}} / \partial r$ in the flow profile. This means that (for example) a plasma will drift upward in the closed field line region, and downward in the open field line region.

This happens simply based on the equilibrium of the plasma: the SOL dynamics are set by the sheath physics, and a radial force balance on the ions just inside the edge. The shear layer between these two regions naturally exists.

To summarize, $\vec{E} \times \vec{B}_o$ shear naturally exists at the LCFS. Drift turbulence (where $|k_{||}| > 0$) exists inside the LCFS, while drift turbulence **and** interchange modes (where $|k_{||}| \sim 0$, but finite $|k_{||}|$ can exist as well) exist in the SOL. Increasing heating will increase the $\vec{E} \times \vec{B}$ shear layer, which follows from the equilibrium physics discussed in this section: increasing heating will increase temperatures, steepen the potential profile, and increase the pressure gradient. Increased damping of $\vec{E} \times \vec{B}$ flow (due to ion-neutral charge exchange giving a momentum sink for the ions, trapped-passing ion collisions, electron collisions, and/or an increase in density n/\bar{n}_G) will lead to a decrease in the gradient of the shear $\partial \vec{v}_E / \partial r$. The existence of a shear layer in confined plasma has been discussed in the previous lecture.

3 PMI: Effect of plasma on the materials

Now that we have discovered what happens at the plasma edge, what does the plasma actually *do* to the material it is coming in contact with, particularly at steady-state in reactor-relevant conditions and time scales?

As we move towards ignition in fusion plasmas, concerns with the interactions between the high temperature plasmas and first-wall materials become significant. This is the study of plasma-material interactions (PMI) or plasma-wall interactions (PWI), which includes plasma physics, materials science, atomic physics, and more. PMI instantly and continuously remakes and remodels the plasma-facing surface, which significantly changes both the material properties and the plasma behavior.

3.1 What's going on?

Plasma ions impinge on the material surface at a finite energy, typically $\sim 100\text{eV}$, and implant into the first 1-100 Angstroms of the material surface, as illustrated in Figure 8. They can come to rest in the material, forming trapped gas, or they can be bounced back into the plasma, typically neutralized and recycled back into the volume as neutral atoms. The ions can also "kick out" atoms of the material surface in a process called physical sputtering. Depending on the material, the plasma can also cause chemical sputtering, where the plasma forms molecules with atoms on the material surface that are released by thermal properties into the plasma. The plasma can also be permanently trapped in the material and form bubbles and blisters, diffuse deep into the material and eventually reach the cooling channels located about a centimeter below the surface, or trapped

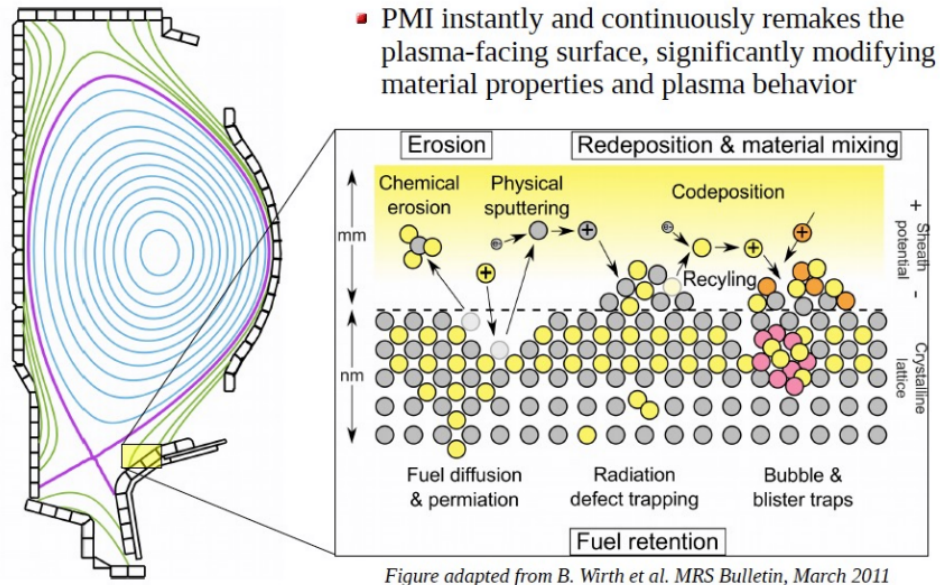


Figure 8: Plasma-material interactions. Gray spheres represent the atoms of the solid material surface, yellow are plasma ions.

in defects in the material created by the fusion neutrons themselves, known as radiation defect trapping. All of these processes lead to the retention of fusion fuel, particularly tritium.

3.2 Where PMI comes in

Reactor-relevant operational conditions will require long-pulse operation that will be several orders of magnitude longer than any present-day fusion device is capable of achieving. There are many, many issues relating to PMI that result from this long-pulse operation, which have been outlined in Figure 9.

3.2.1 Divertor particle and power handling

The single most important, interesting, relevant, criminally underfunded, and overall very best and the most super cool topic in fusion is the divertor, which is responsible for managing heat loads and controlling density. Divertor heat loads force extreme divertor target designs. Divertor targets often have a high-Z refractory material that faces the plasma, with active cooling channels close to the material surface. These cooling channels are tubes embedded about 1cm into the first wall material, below the surface, that run high-pressure helium to the back-face of the plasma-facing surface. These design constraints force a maximum heat flux of $10\text{MW}/\text{m}^2$ that the plasma-facing surface can survive (recall that the plasma exhausts at about $1\text{GW}/\text{m}^2$, which is about 100x the survivable heat flux). With this peak heat flux and a target thickness of a few millimeters, the surface temperature of the divertor target will be between 1200-1500C.

The divertor target must be able to last through many, many long-pulse plasma discharges, but it also must be thin, to maintain contact between the material and the cooling channel. At the divertor target, the particle fluence (or exposure) is approximately 10^{31} ions per square meter over


PMI Issue	Reactor Impact	Research Need	
Divertor particle & power handling	Dissipate divertor thermal loads ,density control	Edge/SOL transport physics; advanced divertors, transient control	 Increasing Timescale
PMI Impact on Confinement	Maintain core plasma performance	Long pulse (1000s seconds) tokamak w/ CFETR relevant wall conditions	
Surface Morphology Evolution	Loss of performance at high heat flux; dust generation	Understand mechanisms & manage/avoid deleterious conditions	
Helium Accumulation	Effect on D/T Retention, Material performance	In-situ real-time diagnostic for He , D content;	
Fuel Retention Probability $\sim 10^{-6}$ - 10^{-7}	TBR>1	In-situ real-time D, T profiles over <10microns;also need He profiles since He affects retention	
Surface Erosion <~ 1mm/year requires $Y_{net}<10^{-5}$	Wall & Divertor Reliability & Lifetime	In-situ diagnostics Sensitive to ~100's nm over 10micron dynamic range	
Material Migration & Mixed Material Formation	Minimize & Predict evolution of mixed materials	2D SOL Plasma Flows; in-situ mixed material diagnostics	
Rad-damage & Transmutation Effects	New (Degraded?) Materials Properties	Neutron surrogates; neutron irradiation; studies of In-situ retention, material properties	

Figure 9: The major PMI-related issues relating to fusion energy production, ordered by increasing timescale. A few of these topics will be covered in this review.

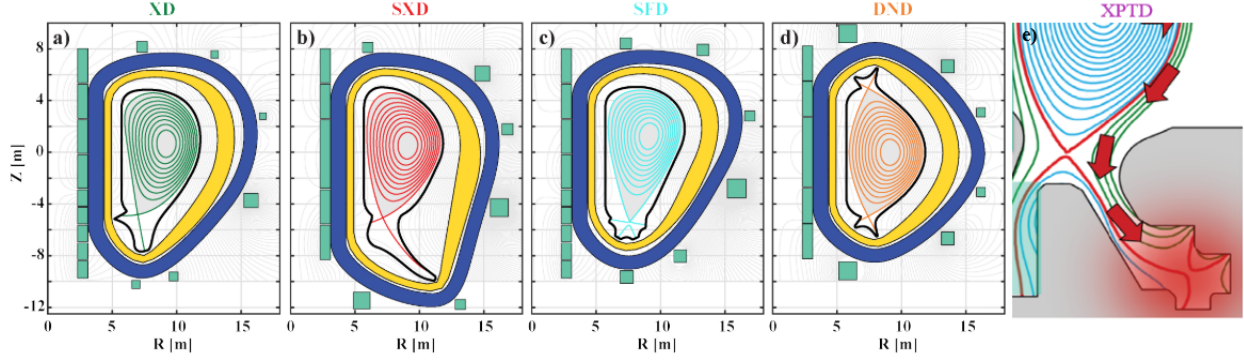


Figure 10: Divertor geometries for various proposed alternative divertor configurations, taken from [11] and [12]. (a) shows the X-Divertor configuration (XD), (b) shows the Super-X Divertor configuration (SXD), (c) shows the Snowflake Divertor Configuration (SFD), (d) shows the Double Null Divertor Configuration (DND), and (e) shows the X-Point Target Divertor configuration (XPTD).

the period of one year. If we allow for 1mm of target erosion per year, then for every ion incident on the target, the probability of that ion eroding an atom of the target material must be approximately 6×10^{-6} , or one in about 10 million, while all other incident ions must not erode any of the target material.

Measured sputtering yields indicate that sputtering increases with incident deuterium ion energy. From the physics of the plasma sheath, we know that the ion energy corresponds to the electron energy, meaning that the electron temperature must be cooled from the midplane value to an acceptable level at the plasma sheath so these erosion events will be less significant. This is an example of how the material limit forces certain plasma conditions: we have to figure out how to cool the plasma electrons so the sputtering is low enough so we have an adequate lifetime for the divertory target.

Reducing electron temperature will require a radiative and/or alternative divertor. Such a design has not been demonstrated yet, and remains an active area of research (the most important area of research in all of everything). Several proposed alternative divertor designs are shown in Figure 10.

One "solution" introduced by these new divertor designs is to expand the magnetic flux surface, which is the technique used in the Snowflake divertor design, shown in Figure 10(b). The Snowflake divertor works via flux expansion, where the magnetic surfaces are expanded through multiple poloidal field shaping coils located below the divertor targets. This enables the $> 1\text{cm}$ wide heat flux channel at the midplane (which we estimated earlier) to expand out to about 10 – 20cm by stretching or pulling the flux surfaces out with these coils.

Another idea is to move the divertor strike points to larger major radius, as in the X-Divertor and Super-X Divertor designs, shown in Figure 10(a) and (b). Normally, the divertor target plates are relatively close to the X-point (as in Figure 10(d), which is a double-null configuration with two standard divertors). The idea with these long-leg divertors is to move the strike plate to much larger radius, which gives time and space for the plasma to diffuse across the magnetic surfaces to spread

the heat flux out over a larger area. The major drawback to this scheme is that a long leg usually requires an expanded divertor chamber, which can be costly; the additional space for the long leg will also require an expansion of the toroidal field that will not be in contact with "useful" plasma, which is hard to justify.

Both of these schemes are being examined via simulations and experiments.

With respect to the recent declarations of victory at MAST-U that they have reached the "solution" to the exhaust problem using a Super-X configuration [13]: this author's semi-professional opinion as a fledgling divertor physicist, shaped by the finest minds from Eastern Europe to be highly skeptical and very pessimistic about everything, is an eyebrow raise, a cigarette flick, and a "*We'll see*". She encourages the Department of Energy to ignore these claims and continue to fund the grant upon which she is paid.

3.2.2 PMI impact on confinement

We need to maintain good plasma performance for very long durations, on the order of hours, days, or weeks of continuous plasma operation. For example, in experiments, the JET tokamak operated with a carbon wall and divertor for the majority of the machine's lifetime, and was able to achieve high edge pedestal temperatures and densities using the carbon configuration. When the walls were switched to an ITER-like configuration using a beryllium first wall and tungsten divertor, they got poorer performance in these edge pedestal temperature and density measurements and other relevant confinement metrics. The reasons for this decline in performance are not yet well-understood, but emphasize that the material does affect core plasma performance.

It is possible to "cheat" the physics by using lithium or boronization, where the walls of the machine are coated with low-Z impurities to try to achieve high performance. This allows for the plasma to achieve record-long H-modes, but is ultimately irrelevant, since these coatings are transient: there has been no feasible way to maintain a long-duration, high-performance plasma with a wall coating that would be relevant for a reactor. We don't understand why these wall coatings have an effect on core plasma performance - it could be due to neutral recycling effect, an effect on pedestal fueling, or some influence of the low-Z material on flow shear, but we don't know for sure.

3.2.3 Surface morphology evolution

Now, we will discuss the effect that the plasma has on the material. When we build a tokamak, great care is taken to build the machine *very* precisely, often to micron precision, and the materials are carefully engineered. Then, this finely-tuned device is exposed to extreme plasma conditions, and all hell breaks loose and severely modifies these carefully designed materials.

Transient heat loads like ELMs can be mimicked in laboratory conditions using a suitably ramped laser pulse to study the effects of these extreme events on the material surfaces. These studies tell us that it's very easy to melt a tungsten divertor target using an ITER-grade, type I ELM.

Other effects of the plasma on materials can be seen in Figure 11, where the surface morphology of many materials has been drastically altered after plasma exposure.

These laboratory experiments seek to assess the material properties in ITER by emulating plasma

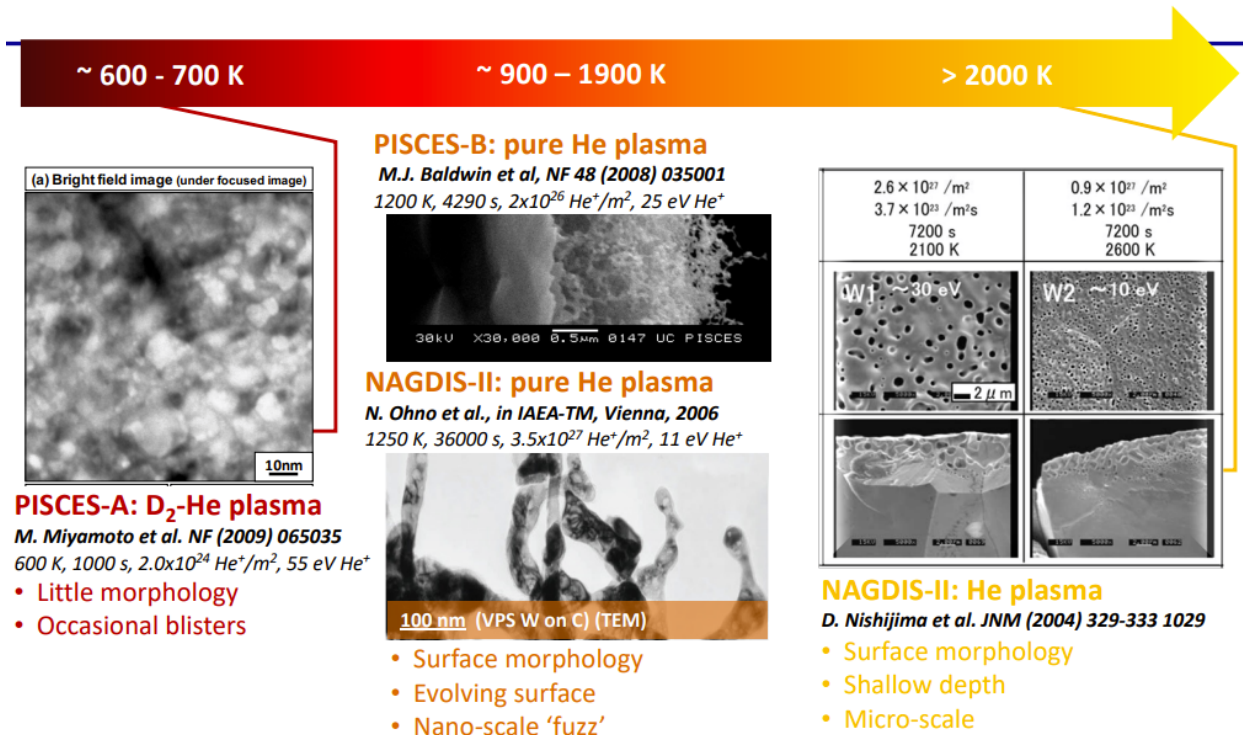


Figure 11: Various materials after being exposed to laboratory plasmas.

conditions expected in the device. In Figure 11(a), a tungsten material surface (like the divertor in ITER) has been exposed to a mixture of deuterium and helium (since in a burning plasma, there will be helium that is escaping from the fusion reaction into the divertor). At low temperatures (600-700K), little bubbles of helium will begin to form in the near-surface region. This looks rather like the foam on top of a glass of beer, where the material surface is like the liquid of the beer and the helium bubbles are like the foam. If the material gets hotter, approaching 1000K, these bubbles now give birth to little tendrils of material that grow out of the bubbles and into the plasma. This layer of "fuzz" is about a micron thick, and what was once shiny, smooth, crystalline tungsten is now a weird-looking, tendril-covered beast, where the ends of the tungsten "fingers" are filled with helium bubbles. Raising the temperature even further to about 2000K (which is not even halfway to the melting point of tungsten), these helium bubbles will congeal and increase in size, with macro- and micro-scale helium bubbles in the material that look like Swiss cheese. This is a diffusive process, and an analytic model can be derived for this phenomenon based on the particle fluence to the target.

3.2.4 Helium accumulation

Another "hot topic" in PMI is helium accumulation and, in particular, the effect on tritium retention in a fusion machine. To license a fusion energy device, the nuclear licensing authorities in the respective countries must be convinced that you will not accumulate too much tritium in the machine, since tritium is a radioactive substance that can be bad if released into the environment

and result in bad PR for the fusion industry. You must be able to predict how much tritium will get stuck in the machine so you will know how much to report to the appropriate authorities.

The other important thing to worry about with tritium retention (aside from safety concerns) is that you can only trap less than one in a million tritium atoms in the wall. Exceeding that tritium trapping probability means that it will be impossible to close the tritium trapping fuel cycle.

The good news about the helium bubble layer that forms in the plasma is that the helium layer acts as a diffusion barrier, or a transport barrier, for the diffusion of hydrogen (as deuterium or tritium) into the material. The physics of this process are not yet well-understood, but this phenomenon has been shown experimentally.

The bad news is neutrons. Neutrons are produced from the fusion reaction, and are released at very high energy, $14MeV$. The mean free path of these neutrons in solid materials is measured in several centimeters. This means that the entire first-wall material and the divertor target will be bathed in a flux of energetic neutrons. These energetic neutrons have an impact on tritium retention, since the neutrals will eventually collide with another atom in the material crystal, and transfer 100s of KeV of kinetic energy to an atom in the crystal lattice via elastic collision. That atom will be kicked out of the lattice, and form a primary knock-on atom, which is actually an ion. Now, there is a $100keV$ ion rattling around in the material, and it collides with its neighbors, transfers energy to them, and forms what is called a "collision cascade". This is where a few displaced atoms will cause a significant displacement in thousands of other atoms in the lattice position, essentially melting the material for a brief moment on the order of 10s of picoseconds. Eventually, the material will lose energy, and most atoms move back into their lattice positions, but some of them that don't fall back into their original positions form an "interstitial vacancy pair", where material atoms can be present or vacant in the lattice in the final state of the material. These vacancies can act as trap sites, meaning deuterium or tritium atoms diffusing through the material can now be trapped in these vacancies left by the atoms in the material lattice.

Understanding tritium retention is very important for the viability of a self-sufficient fusion reactor. Doing a particle balance, shown in the cartoon in Figure 12, we are burning tritium at some rate in the core (\dot{m}_T^{burn} in the core), which releases fusion energy, and some amount of tritium is transported to the wall via turbulent transport (\dot{M}_T^{wall} to the wall). There is a recycling coefficient R , so some portion of the material immediately recycles back into the plasma, and $(1 - R)$ begins to burrow into the wall. The mass balance is shown in the figure; \dot{M}_T^{inj} is the mass of injected tritium into the plasma, while the fueling efficiency term η_{fuel} accounts for losses, since not all injected tritium will make it into the core plasma. The burn probability p_{burn} is very small, and accounts for the fact that only a small amount of tritium will burn. Most of the tritium injected into the system will just churn from the wall to the plasma, back to the wall and back to the plasma, and only occasionally will burn.

The probability of tritium trapped in the wall can be defined by $p_{trap} = \dot{M}_T^{trap} / \dot{M}_T^{wall}$. Then, this probability must be below

$$p_{trap} \ll (TBR - 1)(1 - R) \frac{p_{burn} \eta_{fuel}}{1 - p_{burn} \eta_{fuel}}, \quad (21)$$

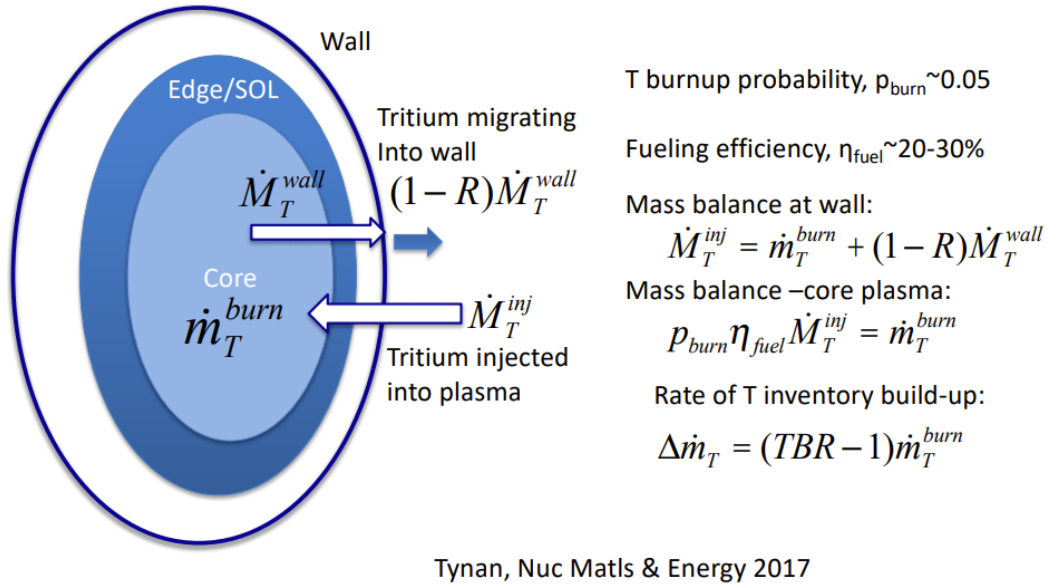


Figure 12: Cartoon and particle balance for tritium retention. The dark blue line is the wall and divertor, and the lighter blue is the plasma. The core plasma is in the lightest blue. From [14].

where TBR is the tritium breeding ratio. Typical numbers, with $TBR \sim 1.05$ and $R \sim 0.99 - 0.999$ give a trapping probability of $p_{\text{trap}} \ll 10^{-6} - 10^{-7}$, below one in a million or below one in ten million.

This means there are two strong cases for tritium inventory control and small tritium retention probability: nuclear safety (and therefore, fusion PR) and closing the tritium fuel cycle.

Experiments studying tritium retention indicate acceptably low retention levels in non-neutron-damaged materials, with even lower retention levels at higher fluences and temperatures due to the impact of the helium layer and embedded particles being able to escape the material at higher temperatures. However, the retention levels are about an order of magnitude higher in neutron-damaged materials. This means that until the protective helium layer can build up on the surfaces and the wall can come to equilibrium (which is estimated to take around 10 weeks), the retention will not be low enough to close the fuel cycle. As a result, tritium must be fed into the system until the walls are saturated enough to sustain the tritium fuel cycle. This is a key issue that must be studied and understood, looking towards ITER and beyond to reactor-relevant conditions. Other pressing issues are detailed in Figure 13.

PMI Issue	Science Question	Possible Approach
Material Erosion	How does high particle flux affect erosion rate?	Implanted depth markers & Ion-beam NRA; Plasma spectroscopy
Material Redeposition	How quickly is material being redeposited, and what type of mixed materials are formed?	Ion-beam NRA, LIBS, Plasma Spectroscopy & 2D imaging
Fuel retention in D, D-T, and D-T/He Plasmas	Is D/T retention low enough for TBR>1?	Ion-beam Rad-damage, NRA, LIBS, Ex-situ TDS
Rad-damage effects on PMI	Are there synergistic PMI/Rad-damage effects? Effects on retention? He effects?	Combined plasma/ion beam studies using He & Heavy Ions; GIXRD
Managing divertor heat flux	How do injected divertor impurities affect material surfaces?	Divertor simulator w/ PMI capabilities

Figure 13: To-do list.

References

- (1) The Edge® Pizza <https://www.pizzahut.com/c/content/the-edge>.
- (2) Krasheninnikov, S. et al. Stability of divertor detachment. *Nuclear Materials and Energy* **2017**, *12*, 1061–1066.
- (3) Krasheninnikov, S. I.; Smolyakov, A.; Kukushkin, A., *On the Edge of Magnetic Fusion Devices*, 1st ed.; Springer: Cham, Switzerland, 2020.
- (4) Krasheninnikov, S. I. et al. Stability of the detachment front in a tokamak divertor. *Journal of Nuclear Materials* **1999**, *266*, 251–257.
- (5) Soukhanovskii, V. A. et al. In *Proceedings - Symposium on Fusion Engineering*, 2016.
- (6) Buttery, R. Tweet. <https://twitter.com/rjbuttery/status/1403217392881352705>.
- (7) Tonks, L.; Langmuir, I. A General Theory of the Plasma of an Arc. *Phys. Rev.* **1929**, *34*, 876–972.
- (8) Hobbs, G. D.; Wesson, J. A. Heat flow through a Langmuir sheath in the presence of electron emission. *Plasma Physics* **1967**, *9*, 85–87.
- (9) Campanell, M. D. Negative plasma potential relative to electron-emitting surfaces. *Phys. Rev. E.* **2013**, *88*, 033103.
- (10) Krasheninnikov, S. Lecture notes in MAE 217A: Introduction to Gas Discharge Plasma Physics, 2018.
- (11) Reimerdes, H. et al. Assessment of alternative divertor configurations as an exhaust solution for DEMO. *Nuclear Fusion* **2020**, *60*, 1–8.
- (12) LaBombard, B. et al. ADX: A high field, high power density, advanced divertor and RF tokamak. *Nuclear Fusion* **2015**, *55*, DOI: [10.1088/0029-5515/55/5/053020](https://doi.org/10.1088/0029-5515/55/5/053020).
- (13) First results from UK experiment point to a solution to one of fusion's hottest problems <https://ccfe.ukaea.uk/first-results-from-uk-experiment-point-to-a-solution-to-one-of-fusions-hottest-problems/>.
- (14) Tynan, G. et al. Deuterium retention and thermal conductivity in ion-beam displacement-damaged tungsten. *Nuclear Materials and Energy* **2017**, *12*, Proceedings of the 22nd International Conference on Plasma Surface Interactions 2016, 22nd PSI, 164–168.